The
University
Of
Sheffield.

This is a repository copy of *Renewable energy sharing among base stations as a min-cost-max-flow optimization problem*.

Renewable Energy Sharing among Base Stations as a Min-Cost-Max-Flow Optimization Problem

Doris Benda, *Student Member, IEEE,* Xiaoli Chu, *Senior Member, IEEE,* Sumei Sun, *Fellow, IEEE,* Tony Q.S. Quek, *Fellow, IEEE,* and Alastair Buckley

Abstract—**Limited work has been done to optimize the power sharing among base stations (BSs) while considering the topology of the cellular network and the distance-dependent power loss (DDPL) in the transmission lines. In this paper, we propose two power sharing optimization algorithms for energy-harvesting BSs: the max-flow (MF) algorithm and the min-cost-max-flow (MCMF) algorithm. The two proposed algorithms minimize the power drawn from the main grid by letting BSs with power surpluses transmit harvested power to BSs with deficits. The MCMF algorithm has an additional DDPL cost associated with each transmission line. Hence, the MCMF algorithm shares the harvested power over shorter distances and loses less power during the transmission than the MF algorithm. Our numerical results show that for a fully connected cellular network, i.e., every pair of BSs can share power, with a moderate power loss coefficient per l ($\in \mathbb{R}^+$) meters of transmission line, the MCMF algorithm saves up to 10%, 22%, and 30% more main grid power than the MF algorithm for 5, 10, and 15 BSs uniformly distributed in a square area of l^2 square meters, respectively.**

Index Terms—**Cellular network, min-cost-max-flow, max-flow, energy harvesting, energy sharing**

I. INTRODUCTION

More than half of the energy consumption in the cellular network infrastructure is caused by the operation of base stations (BSs) [2]. In addition, environmental policies promote the incorporation of environmentally friendly technologies. As a result, BSs equipped with energy-harvesting devices, e.g. solar cells, are becoming increasingly attractive to cellular network operators [3], [4]. Furthermore, cellular networks capable of energy-harvesting are more sustainable and resilient during natural disasters than conventional grid-connected ones [2].

D. Benda, and X. Chu are with the department of Electronic and Electrical Engineering, University of Sheffield, The United Kingdom, e-mail: dcbenda1@sheffield.ac.uk, and x.chu@sheffield.ac.uk.

D. Benda and S. Sun are with the Communications and Networks Cluster, Institute for Infocomm Research, Singapore, e-mail: studcb@i2r.a-star.edu.sg and sunsm@i2r.a-star.edu.sg.

T. Q.S. Quek is with the Information Systems Technology and Design Pillar, Singapore University of Technology and Design, Singapore, e-mail: tonyquek@sutd.edu.sg.

A. Buckley is with the department of Physics and Astronomy, University of Sheffield, The United Kingdom, e-mail: alastair.buckley@sheffield.ac.uk.

A. Different Power Sharing Methods

The amount of harvested power as well as the power consumption of the BSs vary over time and space resulting in power surpluses or power deficits at the BSs. To avoid wasting precious harvested power, power can be transmitted from surplus BSs to deficit BSs via transmission lines. Other options for power sharing are wireless power transfer, traffic offloading to neighboring BSs, smart grid/ main grid trading and batteries. In the following, we will discuss these options separately and compare them with power sharing via direct transmission lines.

1) Wireless Power Transfer: Power can be shared through wireless power transfer. Nonetheless, this is limited to very short distances due to the high power losses associated with long wireless power transmission [5].

2) Traffic Offloading To Neighboring BSs: The authors in [6] propose to offload user equipments (UEs) at the cell edge of BSs with power deficit to neighboring BSs with abundant renewable energy. Nonetheless, this causes a deterioration in the signal-to-interference-plus-noise ratio (SINR) of the offloaded UEs, whereas power sharing via direct transmission lines does not affect the SINR.

3) Smart Grid/ Main Grid Trading: The authors in [7], [8] propose to sell and buy power from the grid and use the grid to conduct virtual power transfer in addition to power sharing via direct transmission lines. Power sharing via direct transmission lines requires high capital expenditure for deploying physical transmission lines whereas grid trading implies operational expenditure in the form of a price that has to paid to the grid operator. To evaluate if the initial investment for deploying physical transmission lines is justified in the long-term or each BS should rather sell and buy its power from the grid, the local price structure has to be evaluated. BSs can buy power from the grid at a price p_b and sell it to the grid at a price p_s, where the grid operator typically requires that $p_b > p_s$. The difference in price denoted by Δ_p is as follows: $\Delta_p = p_b - p_s$. If Δ_p is great, it is more cost efficient to share power via direct transmission lines. If Δ_p is small, it is more cost efficient to sell and buy power from the grid. Even if Δ_p is small, cellular network operators may prefer to rely on their own local power sharing infrastructure to avoid reliance on the grid and to avoid the risk of future power price changes beyond their control. In general, power sharing via direct transmission lines is usually cost efficient in dense cellular networks with small to medium inter-site distances, where the power losses in the transmission lines are low, expensive step-up and step-down

transformers are not needed, and DC to AC conversion losses are negligible if DC transmission lines are deployed between DC energy harvesters such as solar cells. In contrast, sparse cellular networks with long inter-site distances are not suitable for power sharing via direct transmission lines due to the high power loss during transmissions, the high capital expenditure, and the right-of-way clearance needed for the transmission corridors. In the latter case, power will be more likely bought and sold to the grid.

4) Batteries: Since batteries are expensive and have a short lifetime (3-9 years), battery replacements significantly contribute to the system lifetime cost [9]. Employing both, direct transmission lines for power sharing and batteries to balance the mismatch between the power generation and consumption at the BSs would greatly increase the capital expenditure. Hence, we only use direct transmission lines in our system model to reduce the capital expenditure.

B. Justification For Power Surpluses And Deficits At Neighboring BSs

It has been shown that 80% of grid power can be saved if power sharing is enabled between two energy-harvesting BSs with anti-correlated energy profiles [10]. Meanwhile, considering the power loss along the transmission lines, it is preferred to share power among BSs that are not far away from each other. Anti-correlated energy generation profiles at neighboring BSs can be obtained by different types of energy harvesters.

For example, a solar cell and a wind turbine in the same area can achieve anti-correlated energy generation profiles on a daily timescale due to the fact that high (low) pressure areas tend to be sunny (cloudy) with low (high) surface wind, and on a seasonal timescale due to the fact that more solar (wind) energy can be harvested in summer (winter) than in winter (summer) [3]. If only solar cells are available for deployment, anti-correlated energy profiles at neighboring BSs can be achieved by deploying southeast orientated solar cells and southwest orientated solar cells, respectively (cf. Fig. 3 in [4]), where a southeast (southwest) orientated solar cell has an orientation angle of $-45°(45°)$ with respect to the southern direction [4].

Furthermore, even if two BSs have similar energy generation profiles, different traffic loads at the BSs may result in power surpluses and deficits as well, because the power consumption profiles at the BSs are traffic load-dependent and can be different (cf. [11]).

C. Background Of The Used Optimization Algorithms

We propose two power sharing optimization algorithms based on the max-flow (MF) problem and the min-cost-max-flow (MCMF) problem, which are well known for their low computational complexity. For a flow network with $|E|$ edges and $|V|$ vertices, the MF problem and the MCMF problem can be efficiently solved in $\mathcal{O}(|V|^2|E|)$ (general push-relabel algorithm [12]) and $\mathcal{O}(|E|\log|E|(|E|+|V|\log|V|))$ (Orlin's algorithm [13]), respectively. In practice, network simplex

algorithms are commonly used to solve the MF problem and the MCMF problem as well [13].

D. Current Knowledge Gaps

There are three main issues that have not been sufficiently studied in the current literature:

1) Distance-dependent Power Loss In Transmission Lines: Transmitting power over longer distances will result in higher resistive power losses, but most existing works do not include distance-dependent power loss (DDPL) in their system model. For example, [14] introduced an energy hub for power sharing in cellular networks and assumed that the resistive power loss in the transmission lines is independent of the power propagation distance.

2) Topology Of The Cellular Network: Most existing works consider sharing power among only a few BSs, e.g., two BSs in [10] and three BSs in [8], without systematically considering the topology of the cellular network. In this paper, we generalize the BS power sharing scenario to a dense cellular network, where the topology of the cellular network is incorporated in the system model and the harvested renewable power is shared among nearby BSs.

3) Performance Gain vs. Complexity Of Power Loss Aware Power Sharing Algorithms: To the best of our knowledge, this work is the first to investigate the trade-off between the performance gain and the computational complexity of BS power sharing algorithms with or without considering the transmission line power loss. Moreover, the main difference to [7] is that we evaluate the performance gains that a power loss aware power sharing algorithm can achieve in different cellular networks and derive guidelines on power loss aware power sharing for different cellular network deployment scenarios.

E. Contributions

The main contributions of this paper address the identified knowledge gaps as follows:

- We propose a BS power sharing model for energy-harvesting enabled dense cellular networks and incorporate into the BS power sharing model the topology of the cellular network and the DDPL in the transmission lines.
- We develop an MF algorithm and an MCMF algorithm which both minimize the power drawn from the main grid by letting BSs with surpluses transmit harvested power to BSs with deficits. The MCMF algorithm has an additional DDPL cost associated with each transmission line and therefore reduces the power losses during the transmission.
- We derive a closed-form expression of the average total power drawn from the main grid by all the BSs for the MF algorithm on a complete neighboring graph. The accuracy of the closed-form expression is verified by the simulation results.
- We investigate the performance gap between the two proposed algorithms for different DDPL values, different BS densities, different maximum power surpluses/deficits at the BSs, and different power surplus/deficit distributions.

Based on the insights obtained, we provide guidelines on which of the two algorithms should be used under different scenarios of energy-harvesting enabled cellular networks.

The rest of this paper is organized as follows. Section II presents the system model. Section III formulates the MF/MCMF problem. Section IV proposes a linear optimization program to solve the MF/MCMF problem. Section V derives a closed-form expression of the average total power drawn from the main grid by the BSs for the MF algorithm. Section VI presents the performance evaluation results for both algorithms. Finally, the paper is concluded in Section VII.

II. SYSTEM MODEL

We consider $N \in \mathbb{N}$ uniformly distributed BSs in a square area of l^2 square meters (cf. Fig. 1), which are denoted as BS_i, $i \in \{1, ..., N\}$. Each BS is equipped with an energy-harvesting device, e.g., a solar cell, as well as a main grid connection but no battery.

We denote the power surplus/deficit of BS_i as $B_i[\text{W}]$ in watts. A surplus (deficit) in power at BS_i is indicated by a positive (negative) value B_i. The objective is to balance out the power in the network by transmitting power from surplus BSs to deficit BSs so that the total power drawn from the main grid by the deficit BSs is minimized. A BS_i with $B_i = 0$ will not take part in the power sharing scheme.

The set of surplus BSs is denoted as BS^+, and the set of deficit BSs is denoted as BS^-, i.e.,

$$BS^+ = \{i \,|\, B_i > 0, \ i \in \{1, ..., N\}\},$$
$$BS^- = \{i \,|\, B_i < 0, \ i \in \{1, ..., N\}\}. \tag{1}$$

For the network, the total power surplus B^+, the total power deficit B^-, and the net power surplus/deficit B^{net} are given by

$$B^+ = \sum_{i \in BS^+} B_i,$$
$$B^- = \sum_{i \in BS^-} B_i, \tag{2}$$
$$B^{\text{net}} = \sum_{i=1}^{N} B_i = B^+ + B^-.$$

BSs can be connected by a transmission line in a cellular network. As depicted in Fig. 2, the network is represented by a neighboring graph, where vertices denote BSs and edges denote transmission lines. Two BSs can share power between each other only if they are connected by an edge. BSs that are connected by an edge are referred to as neighboring BSs.

Sharing power between two BSs will result in some power loss as heat along the transmission line known as resistive heating. The power loss $P_{\text{loss}}[\text{W}]$ in watts in the transmission line can be calculated by Ohm's law and the formula for the transmission line resistance [15] as follows:

$$P_{\text{loss}} = I^2 \cdot \rho \cdot \frac{d}{A_{\text{c}}}, \tag{3}$$

where $I[\text{A}]$ in amperes represents the current traveling through the transmission line, $\rho[\Omega\text{m}]$ in ohm-meters represents the resistivity of the transmission line, $d[\text{m}]$ in meters represents the length of the transmission line, and $A_{\text{c}}[\text{m}^2]$ in square meters represents the cross-sectional area of the transmission line.

The power loss in the transmission line is proportional to its length as seen in (3). The power loss coefficient $L(i, j)[\Omega]$ in ohms of the edge between BS_i and BS_j is defined as

$$L(i, j) = \min(1, \frac{||BS_i - BS_j||}{l} \cdot C), \tag{4}$$

where $||BS_i - BS_j||[\text{m}]$ in meters is the Euclidean distance between BS_i and BS_j, $l[\text{m}]$ in meters is the side length of the square in Fig. 2, and $C[\Omega]$ in ohms is the power loss coefficient per l meters of transmission line, which encapsulates the constants from (3) as $C = \frac{\rho \cdot l}{A_{\text{c}}}$. $L(i, j)$ is truncated to 1 because it is not possible to lose more than the available power.
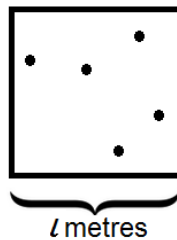

Fig. 1: Illustration of the considered cellular network, with $N = 5$ BSs uniformly distributed in a square area of l^2 square meters.
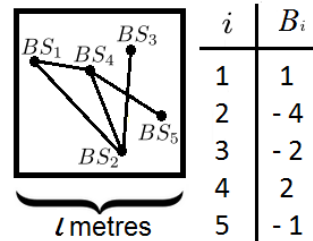
Fig. 2: The neighboring graph representation of the cellular network with example surplus/deficit power parameters B_i given for the BSs.

III. THE MF/MCMF PROBLEM

We use the notation (i, j) to denote the edge between the surplus BS_i and the deficit BS_j, where $(i, j) \in E_n$ indicates that BS_i and BS_j are connected by a transmission line, and the notation $f_{[\text{W}]}\big((i, j)\big)[\text{W}]$ and $f_{[\text{A}^2]}\big((i, j)\big)[\text{A}^2]$ for the power flow and the second power of the current flow on the edge from the surplus BS_i to the deficit BS_j, respectively.

A. Optimization Objective

Resistive heating is caused by the electric current of the power flow in the transmission line but not by the electric potential. Nonetheless, it is out of the scope of this paper to model the relationship between the power and the electric current in the transmission line. Thus, we assume for simplicity that the power flow in the transmission line is equivalent to the second power of the current flow in the transmission line. In other words, a power flow in the transmission line of x watts, is equivalent to a current flow in the transmission line of $I = \sqrt{x}$ amperes in our system model. Hence, $f_{[\text{W}]}\big((i, j)\big)$ and $f_{[\text{A}^2]}\big((i, j)\big)$ have the same quantitative value for every edge (i, j) but their units are different.

The optimization objective is to minimize the total power $M[\text{W}]$ in watts drawn from the main grid by the deficit BSs as follows:

$$M = \min_{f}\left\{\sum_{j\in BS^-}|B_j| - \sum_{\substack{i\in BS^+\\j\in BS^-\\(i,j)\in E_n}} f_{[\mathrm{W}]}\big((i,j)\big) + \underbrace{\sum_{\substack{i\in BS^+\\j\in BS^-\\(i,j)\in E_n}} L(i,j)f_{[\mathrm{A}^2]}\big((i,j)\big)}\right\}$$

$$\underbrace{\hspace{5cm}}_{\substack{M_1\\\text{deficit power that}\\\text{cannot be balanced out}}}\quad\underbrace{\hspace{4cm}}_{\substack{M_2\\\text{power loss in}\\\text{transmission lines}}}$$

(5)

subject to

Power flow out of the surplus BSs:

$$B_i \geq \sum_{\substack{j\in BS^-\\(i,j)\in E_n}} f_{[\mathrm{W}]}\big((i,j)\big)\quad \forall i\in BS^+ \tag{6}$$

Power flow into the deficit BSs:

$$|B_j| \geq \sum_{\substack{i\in BS^+\\(i,j)\in E_n}} f_{[\mathrm{W}]}\big((i,j)\big)\quad \forall j\in BS^-. \tag{7}$$

There are two scenarios in which a deficit BS_i has to draw power from the main grid. On the one hand, a deficit BS_i may not have neighboring surplus BSs that have sufficient power to balance out the power deficit B_i. On the other hand, even if the neighboring surplus BSs have sufficient power to balance out the power deficit B_i, due to the power losses in the transmission lines, the received power at the deficit BS_i is below the required deficit power B_i, so that the deficit BS_i has to offset this difference by drawing main grid power.

B. Definition Of The Flow Network

In the following subsections, we will show the conversion of the neighboring graph (cf. Fig. 2) and the optimization objective (cf. (5)-(7)) into a corresponding flow network G and a corresponding MF/MCMF problem (cf. (14)-(17)), respectively. The optimization objective in form of an MF/MCMF problem can then be efficiently solved. The conversion steps in Figs. 3(a)-3(e) depict the conversion of Fig. 2 into a flow network as an example. The flow network G is represented by the 4-tuple $(V, E, \mathrm{s}, \mathrm{t})$, where V, E, s, and t denote the set of vertices, the set of edges, the source vertex, and the sink vertex of the flow network, respectively. We use the notation $e = (i, j)$ to represent the directed edge e from vertex i to vertex j in the flow network.

1) Edges And Vertices (cf. Fig. 3(a)): Each surplus BS is connected from the source vertex to the surplus BS by a directed edge. These edges are denoted as source edges E_{s}. Each deficit BS is connected from the deficit BS to the sink vertex by a directed edge. These edges are denoted as sink edges E_{t}. If an edge exists between a surplus BS and a deficit BS in the neighboring graph, then the edge is replaced by a directed edge from the surplus BS to the deficit BS in the flow network. These edges are denoted as transmission edges E_{BS}. We do not allow power hopping in our system model

for simplicity[1]. The edges and vertices in the flow network are defined as follows:

$$\begin{aligned}
E_{\mathrm{s}} &= \{(\mathrm{s}, j)\,|\,j\in BS^+\},\\
E_{\mathrm{t}} &= \{(i, \mathrm{t})\,|\,i\in BS^-\},\\
E_{\mathrm{BS}} &= \{(i, j)\,|\,(i, j)\in E_n; i\in BS^+; j\in BS^-\},\\
E &= E_{\mathrm{s}}\cup E_{\mathrm{t}}\cup E_{\mathrm{BS}}\cup (\mathrm{s}, \mathrm{t}),\\
V &= \{1, 2, ..., N\}\cup \mathrm{s}\cup \mathrm{t}.
\end{aligned} \tag{8}$$

The power transmitted from BS_i to BS_j is modeled as a flow along the path $\mathrm{s} - BS_i - BS_j - \mathrm{t}$ in the flow network. To complete the conversion into a flow network, edge capacities $u(e)$, edge costs $c^{MF}(e)$ of the MF algorithm, edge costs $c^{MCMF}(e)$ of the MCMF algorithm and vertex supplies/deficits $b(v)$ will be defined in the following subsections.
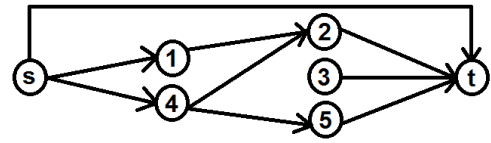
(a) Definition of edges and vertices
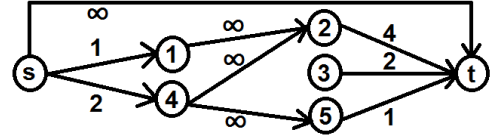
(b) Definition of the edge capacity $u(e)$
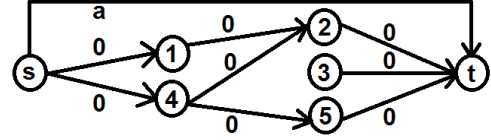
(c) Definition of the edge cost $c^{MF}(e)$
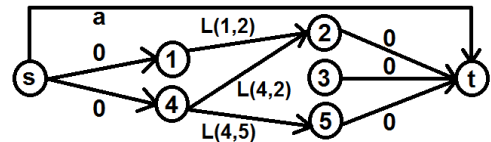
(d) Definition of the edge cost $c^{MCMF}(e)$
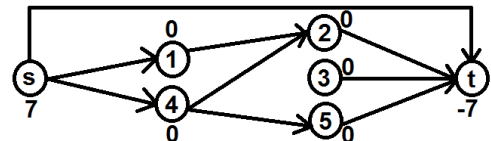
(e) Definition of the vertex supply/deficit $b(v)$

Fig. 3: Conversion of the neighboring graph in Fig. 2 into a flow network

---

[1]If power hopping is considered in the system model, i.e., power can be transmitted from a surplus BS via another BS to a deficit BS, then an edge in the neighboring graph that connects two BSs in BS^+ or that connects two BSs in BS^- is replaced by two directed edges of opposite directions in the flow network.

2) Edge Capacity $u(e)$ (cf. Fig. 3(b)): The capacity $u(e)$ of an edge e represents the maximum power that can pass through this edge. In compliance with (6) and (7), we set the capacities of the edges $e = (\mathrm{s}, j)$ ($j \in BS^+$) to B_j and the capacities of the edges $e = (i, \mathrm{t})$ ($i \in BS^-$) to $|B_i|$. We assume that the power generated by a typical energy-harvesting device at a BS is relatively small with respect to the capacity of a typical transmission line. Hence, the capacities of the transmission edges are set to infinity for simplicity. The edge capacity is thus given by

$$u(e = (i,j)) = \begin{cases} B_j & e \in E_{\mathrm{s}} \\ |B_i| & e \in E_{\mathrm{t}} \\ \infty & e \in E_{\mathrm{BS}}. \end{cases} \qquad (9)$$

3) Edge Cost $c^{MF}(e)$ Of The MF Algorithm (cf. Fig. 3(c)): The MF algorithm is unaware of the distance-dependent power loss in the transmission line. Hence, the cost $c^{MF}(e)$ of transmitting power on the edge e is set to 0 for all edges independent of the distance of the transmission line represented by edge e. The edge cost is given by

$$c^{MF}(e) = 0 \qquad e \in E_{\mathrm{s}} \cup E_{\mathrm{t}} \cup E_{\mathrm{BS}}. \qquad (10)$$

4) Edge Cost $c^{MCMF}(e)$ Of The MCMF Algorithm (cf. Fig. 3(d)): The MCMF algorithm is aware of the distance-dependent power loss in the transmission line. Hence, the cost $c^{MCMF}(e)$ of an edge e represents the power loss in the transmission line due to resistive heating. The costs of the virtual edges in E_{s} as well as in E_{t} are set to 0. The cost of the transmission edge from BS_i to BS_j is equivalent to the power loss coefficient $L(i,j)$ in the transmission line defined in (4). The edge cost is given by

$$c^{MCMF}(e = (i,j)) = \begin{cases} 0 & e \in E_{\mathrm{s}} \cup E_{\mathrm{t}} \\ L(i,j) & e \in E_{\mathrm{BS}}. \end{cases} \qquad (11)$$

5) Vertex Supply/Deficit $b(v)$ (cf. Fig. 3(e)): The vertex supply/deficit $b(v)$ of a vertex v represents the net power flow out or into the vertex. All deficit BSs together require $|B^-|$ watts, therefore $b(\mathrm{t})$ is set to B^-. The $b(\mathrm{s})$ value of the source vertex is set to $|B^-|$ because, even if the supply is greater, the sink does not need more than $|B^-|$ watts. The supply/deficit values of all other vertices are set to 0 because they pass on the power flow from the source to the sink. The definition of the vertex supply/deficit is summarized as follows:

$$b(v) = \begin{cases} B^- & v = \mathrm{t} \\ |B^-| & v = \mathrm{s} \\ 0 & v \in V \setminus \{\mathrm{s}, \mathrm{t}\}. \end{cases} \qquad (12)$$

6) (s, t) Edge (cf. Figs. 3(a)-3(e)): The maximum value of an s-t-flow is equal to the minimum capacity of an s-t-cut in a flow network [16]. Due to the supply/deficit value of the source s and the sink t, the maximum flow value in the defined flow network is smaller or equal to $|B^-|$. The maximum flow value is smaller if and only if a minimum cut with capacity smaller than $|B^-|$ exists.

We can ensure that the maximum flow value always equals $|B^-|$ by adding a virtual (s, t) edge connecting the source

and sink directly with a capacity of infinity and a cost of $a > 1$ ($a \in \mathbb{N}$). This virtual edge ensures that no minimum cut with capacity smaller than $|B^-|$ would occur. The trivial flow of passing $|B^-|$ watts through this virtual edge is a feasible flow. Therefore, any other maximum flow will have a maximum flow value of $|B^-|$ as well. The purpose of this virtual edge is to solve the MF/MCMF problem with the linear program described in Section IV, which requires that the complete flow of $|B^-|$ watts can be passed through the network.

Because every $\mathrm{s}-BS_i-BS_j-\mathrm{t}$ path has a cost of smaller or equal to 1, the MF/MCMF algorithm only passes flow over the virtual (s, t) edge when there is no other possible path to pass it through the network. Hence, the flow through this virtual edge represents the deficit power, which cannot be balanced out, and thus has to be drawn from the main grid.

There are two reasons why power cannot be balanced out. On the one hand, the total power surplus (B^+) may be smaller than the total power deficit ($|B^-|$). On the other hand, the flow network could be sparse, so that some deficit BSs may not have neighboring surplus BSs that have sufficient power to balance out their power deficit (cf. BS_3 in Fig. 3(b)).

The definition of the (s, t) edge is summarized as follows:

$$\begin{aligned} u(e = (\mathrm{s}, \mathrm{t})) &= \infty, \\ c^{MF}(e = (\mathrm{s}, \mathrm{t})) &= c^{MCMF}(e = (\mathrm{s}, \mathrm{t})) = a > 1 \ (a \in \mathbb{N}). \end{aligned} \qquad (13)$$

IV. Optimizing The MF/MCMF Problem

We use the Graph::minCost(Graph G) function implemented in the MuPAD notebook of the Symbolic Math Toolbox in MATLAB to solve the MF/MCMF problem. More specifically, it solves the following linear programming problem given as:

$$f^* = \arg \min_f \left\{ \sum_{e \in E} c^x(e) \cdot f_{[\mathrm{A}^2]}(e) \right\} \qquad (14)$$

subject to

Capacity constraints:

$$f_{[\mathrm{W}]}(e) \le u(e), \quad \forall e \in E \qquad (15)$$

Skew symmetry:

$$f_{[\mathrm{W}]/[\mathrm{A}^2]}(e = (i,j)) = -f_{[\mathrm{W}]/[\mathrm{A}^2]}(-e = (j,i)), \quad \forall e \in E \qquad (16)$$

Flow conservation and required flow:

$$\sum_{\substack{j \in V \\ e \in E \text{ or } -e \in E}} f_{[\mathrm{W}]}(e = (i,j)) = b(i), \quad \forall i \in V, \qquad (17)$$

where $e \in E$, $i, j \in V$, s is the source vertex, t is the sink vertex, $f_{[\mathrm{W}]}(e)$ and $f_{[\mathrm{A}^2]}(e)$ are the power flow and the second power of the current flow on the edge e, respectively, $c^x(e)$ is the cost of edge e, i.e., $c^x(e) = c^{MF}(e)$ and $c^x(e) = c^{MCMF}(e)$ for the MF algorithm and MCMF algorithm, respectively, $u(e)$ is the capacity of edge e, and $b(i)$ is the supply/deficit of vertex i.

A. Remarks On The Output Of The MF Algorithm

Because every $s - BS_i - BS_j - t$ path has the same cost of 0 in (10), the flow f^* generated by (14)-(17) is a random maximum flow on the flow network G. The flow $f^*_{[W]}(e)$ over the transmission edge $e = (i,j) \in E_{BS}$ represents the flow of $f^*_{[W]}(e)$ watts from BS_i to BS_j. The total power drawn from the main grid by the deficit BSs of the MF algorithm is denoted as $M^{MF}[W]$ and is calculated by using the distance-dependent cost function $c^{MCMF}(e)$ together with the random maximum flow f^* generated by (14)-(17). It consists of the power passing through the virtual (s,t) edge denoted as $M_1^{MF}[W]$, and the power lost in the transmission lines denoted as $M_2^{MF}[W]$, i.e.,

$$M^{MF} = \underbrace{f^*_{[W]}(e = (s,t))}_{M_1^{MF}} + \underbrace{\sum_{e \in E \backslash (s,t)} c^{MCMF}(e) \cdot f^*_{[A^2]}(e)}_{M_2^{MF}}.$$

$$(18)$$

Because every $s - BS_i - BS_j - t$ path has a cost of 0 in (10), the MF algorithm only passes flow over the virtual (s,t) edge when there is no other possible path to pass it through the network. Hence, $M_1^{MF}[W]$ and $M_2^{MF}[W]$ in (18) are denoted in accordance with M_1 and M_2 in (5). We want to point out that the cost function $c^{MF}(e)$ has to be used in (14) whereas the cost function $c^{MCMF}(e)$ has to be used in (18).

B. Remarks On The Output Of The MCMF Algorithm

The output of the MCMF algorithm is the optimal power flow f^* over all edges in the flow network G so that the power travels over the shortest distances in the cellular network. The optimal power flow $f^*_{[W]}(e)$ over the transmission edge $e = (i,j) \in E_{BS}$ represents the optimal flow of $f^*_{[W]}(e)$ watts from BS_i to BS_j.

The original optimization objective (5) is equivalent to (19), which calculates the total power drawn from the main grid by the BSs of the MCMF algorithm denoted as $M^{MCMF}[W]$. It consists of the power passing through the virtual (s,t) edge denoted as $M_1^{MCMF}[W]$, and the power lost in the transmission lines denoted as $M_2^{MCMF}[W]$, i.e.,

$$M^{MCMF} = \underbrace{f^*_{[W]}(e = (s,t))}_{M_1^{MCMF}} + \underbrace{\sum_{e \in E \backslash (s,t)} c^{MCMF}(e) \cdot f^*_{[A^2]}(e)}_{M_2^{MCMF}}.$$

$$(19)$$

We want to point out that the cost function $c^{MCMF}(e)$ has to be used in (14) as well as (19).

C. Performance Gap

The performance gap Δ and the relative performance gap $\Delta_\%$ between the two proposed algorithms are defined as follows:

$$\Delta = M^{MF} - M^{MCMF}$$
$$\Delta_\% = \frac{M^{MF} - M^{MCMF}}{M^{MF}}. \qquad (20)$$

Based on the insights obtained in Section VI, we will provide guidelines on which of the two algorithms should be used under different scenarios of energy-harvesting enabled cellular networks.

V. PERFORMANCE ANALYSIS

We analyze the performance of the MF algorithm in this section. In particular, the average drawn main grid power M^{MF} on an edgeless neighboring graph, the average power flow on the (s,t) edge M_1^{MF} on a complete neighboring graph, and the average power loss in the transmission lines M_2^{MF} on a complete neighboring graph, are analytically derived. An edgeless neighboring graph and a complete neighboring graph correspond to no pair of BSs and every pair of BSs is connected by a transmission line, respectively. The superscript ENG and CNG are added to the parameters if an edgeless neighboring graph and a complete neighboring graph are used, respectively. The subscript $_{ana}$ is added to the parameters if the parameters are calculated by a closed-form expression presented in this Section.

We assume that the B_i values are discretely uniformly distributed[2] in the set $\{-B, -B+1, ..., B-1, B\}$, $B \in \mathbb{N}$. As a result, the probability that BS_i experiences a surplus/deficit of p watts is given by

$$P(B_i = p) = \frac{1}{2B+1}, \qquad p \in \{-B, -B+1, ..., B\}.$$

$$(21)$$

A. Analytical Calculation Of $M_{ana}^{MF\_ENG}$ On An Edgeless Neighboring Graph

$M_{ana}^{MF\_ENG}$ corresponds to the average drawn main grid power in a network where no pair of BSs is connected by a transmission line. Because the B_i parameters follow the same probability distribution at all BSs, we can use the example BS_i to calculate the average power deficit of this BS and multiply the result by the number of BS in the network. $M_{ana}^{MF\_ENG}$ can be calculated by summing up the products of each probability of B_i having a negative integer value $p \in \mathbb{N}^-$ and multiply each of these probabilities by the absolute value of p. The explicit expression of $P(B_i = p)$ is given in (21). $M_{ana}^{MF\_ENG}$ can be calculated as follows:

$$M_{ana}^{MF\_ENG} = N \cdot \sum_{p \in \mathbb{N}^-} |p| \cdot P(B_i = p) \stackrel{(21)}{=}$$
$$N \cdot \sum_{p=1}^{B} p \cdot \frac{1}{2B+1}.$$

$$(22)$$

B. Analytical Calculation Of $M_{\text{ana\_1}}^{\text{MF\_CNG}}$ On A Complete Neighboring Graph

$M_{\text{ana\_1}}^{\text{MF\_CNG}}$ corresponds to the average power flow, which cannot be balanced out in the network and therefore flows on the virtual (s, t) edge. We sum up the products of each probability of B^{net} having a negative integer value $p \in \mathbb{N}^-$ and multiply each of these probabilities by the absolute value of p. The second sum in (23) ranges from 1 to BN because B^{net} is the sum of N discretely uniformly distributed parameters on the set $\{-B, -B+1..., B\}$. $M_{\text{ana\_1}}^{\text{MF\_CNG}}$ can be calculated as follows:

$$M_{\text{ana\_1}}^{\text{MF\_CNG}} = \sum_{p \in \mathbb{N}^-} |p| \cdot P(B^{\text{net}} = p) = \sum_{p=1}^{BN} p \cdot P(B^{\text{net}} = -p).$$
(23)

The next paragraph derives a closed-form expression of the probability $P(B^{\text{net}} = -p)$. The generation of B^{net} can be seen as throwing a $(2B+1)$-sided die N times and summing up the number of pips. The number of pips on the die ranges from $-B$ to B. There are in total $(2B + 1)^N$ possibilities of throwing such a die N times. The question is, how many of these possibilities have $-p$ as the sum of the number of pips. This question is equivalent to finding the coefficient $a_{-p+BN+N}$ of the polynomial $(x + x^2 + x^3 + ... + x^{2B+1})^N$ when it is converted into its general form $\sum_{i=0}^{n} a_i x^i$. The conversion of the polynomial is given as

$$\left(x + x^2 + x^3 + ... + x^{2B+1}\right)^N = \sum_{i=N}^{(2B+1)N} a_i x^i$$
(24)

The closed-form expression of the coefficients a_i, $i \in \{N, ..., (2B+1)N\}$, is derived from [17] and given as

$$a_i = \sum_{k=0}^{\lfloor \frac{i-N}{2B+1} \rfloor} (-1)^k \cdot \binom{N}{k} \cdot \binom{i-1-(2B+1)k}{N-1},$$
(25)

where the expression $\binom{n}{k}$ denotes the binomial coefficient "n choose k".

Out of the total number of possibilities of throwing our $(2B+1)$-sided die N times, $a_{-p+BN+N}$ possibilities have $-p$ as the sum of the number of pips. As a result, the probability $P(B^{\text{net}} = -p)$ can be calculated by dividing $a_{-p+BN+N}$ by the total number of possibilities $(2B + 1)^N$ as follows:

$$P(B^{\text{net}} = -p) = \frac{a_{-p+BN+N}}{(2B+1)^N},$$
(26)

where $a_{-p+BN+N}$ is given in (25).

C. Analytical Calculation Of $M_{\text{ana\_2}}^{\text{MF\_CNG}}$ On A Complete Neighboring Graph

$M_{\text{ana}}^{\text{MF\_ENG}} - M_{\text{ana\_1}}^{\text{MF\_CNG}}$ corresponds to the average power flow shared in the cellular network, which is then subject to

power loss in the transmission lines. $M_{\text{ana\_2}}^{\text{MF\_CNG}}$ calculates this power loss in the transmission lines on a complete neighboring graph as follows:

$$M_{\text{ana\_2}}^{\text{MF\_CNG}} = (M_{\text{ana}}^{\text{MF\_ENG}} - M_{\text{ana\_1}}^{\text{MF\_CNG}})$$
$$\cdot \int_0^{\sqrt{2}} P\left(\frac{||BS_i - BS_j||}{l} = x\right) \cdot L(i,j) dx,$$
(27)

where $P\left(\frac{||BS_i - BS_j||}{l} = x\right)$ is the probability density function of the normalized Euclidean distance between the two uniformly distributed random BS_i and BS_j in a square area of l^2 square meters, and $L(i, j)$ is the power loss coefficient on the edge between the BS_i and BS_j. The integral ranges from 0 to $\sqrt{2}$ because $\frac{||BS_i - BS_j||}{l}$ ranges from 0 to $\sqrt{2}$ in a square area of l^2 square meters.

The probability density function[3] of $P\left(\frac{||BS_i - BS_j||}{l} = x\right)$ is derived from [21] and shown in (28)-(29) and Fig. 4 as follows:

$$P_{\text{low}}(x) = 2x(x^2 - 4x + \pi),$$
$$P_{\text{high}}(x) = 2x(4\sqrt{x^2 - 1} - (x^2 + 2 - \pi)$$
$$- 4\tan^{-1}(\sqrt{x^2 - 1})),$$
(28)

$$P(x) = \begin{cases} P_{\text{low}}(x) & 0 \le x \le 1 \\ P_{\text{high}}(x) & 1 \le x \le \sqrt{2} \\ 0 & \text{otherwise.} \end{cases}$$
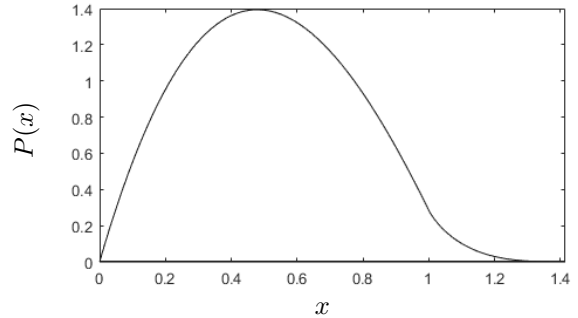(29)

Fig. 4: Probability density function $P(x)$ of the normalized Euclidean distance $\frac{||BS_i - BS_j||}{l} = x$ between the two uniformly distributed random BS_i and BS_j in a square area of l^2 square meters. $P(x)$ is known in the literature as Square-Line-Picking [21].

Because $P\left(\frac{||BS_i - BS_j||}{l} = x\right)$ as well as $L(i, j)$ have different definitions on different domains, it is easier to split the integral (27) and to consider the three cases $0 < \frac{1}{C} \le 1$, $1 \le \frac{1}{C} \le \sqrt{2}$ and $\sqrt{2} \le \frac{1}{C}$ separately:

---

[3]The probability density function for other areas such as rectangular areas, hexagonal areas, and regular polygons have been obtained in [18]–[20].

Case 1: $0 < \frac{1}{C} \leq 1$

$$M_{\text{ana\_2}}^{\text{MF\_CNG}} = (M_{\text{ana}}^{\text{MF\_ENG}} - M_{\text{ana\_1}}^{\text{MF\_CNG}})$$
$$\cdot \left(\int_0^{\frac{1}{C}} P_{\text{low}}(x) \cdot x \cdot C \quad dx \right.$$
$$+ \int_{\frac{1}{C}}^1 P_{\text{low}}(x) \quad dx \tag{30}$$
$$\left. + \int_1^{\sqrt{2}} P_{\text{high}}(x) \quad dx \right)$$

Case 2: $1 \leq \frac{1}{C} \leq \sqrt{2}$

$$M_{\text{ana\_2}}^{\text{MF\_CNG}} = (M_{\text{ana}}^{\text{MF\_ENG}} - M_{\text{ana\_1}}^{\text{MF\_CNG}})$$
$$\cdot \left(\int_0^1 P_{\text{low}}(x) \cdot x \cdot C \quad dx \right.$$
$$+ \int_1^{\frac{1}{C}} P_{\text{high}}(x) \cdot x \cdot C \quad dx \tag{31}$$
$$\left. + \int_{\frac{1}{C}}^{\sqrt{2}} P_{\text{high}}(x) \quad dx \right)$$

Case 3: $\sqrt{2} \leq \frac{1}{C}$
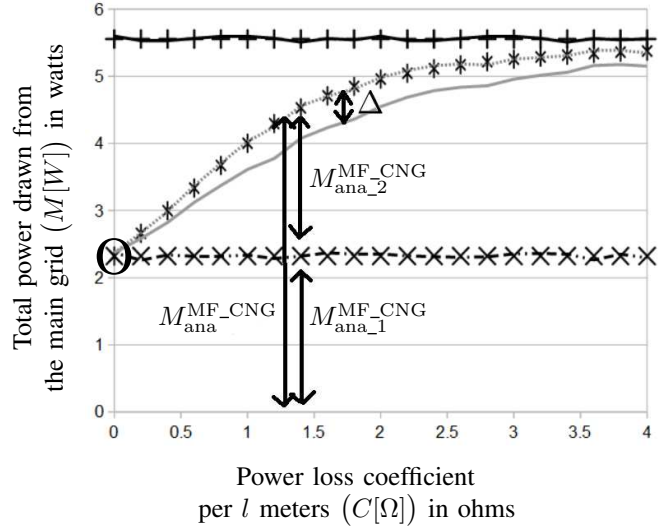
$$M_{\text{ana\_2}}^{\text{MF\_CNG}} = (M_{\text{ana}}^{\text{MF\_ENG}} - M_{\text{ana\_1}}^{\text{MF\_CNG}})$$
$$\cdot \left(\int_0^1 P_{\text{low}}(x) \cdot x \cdot C \quad dx \right.$$
$$\left. + \int_1^{\sqrt{2}} P_{\text{high}}(x) \cdot x \cdot C \quad dx \right) \tag{32}$$

VI. RESULTS

If not stated differently, we use a BS density of $N = 5$ BSs in a square area of l^2 square meters, a maximum power surplus/deficit of $B = 4$, and a power loss coefficient per l meters of $C \in \{0, 0.2, ..., 3.8, 4\}$ to evaluate the performance of the two proposed algorithms. Both algorithms are run 10000 times to derive their average performance.

We use the normalized Euclidean distance $\frac{||BS_i - BS_j||}{l}$ in all formulas, derived parameters and the algorithms. Hence, the results in Figs. 5 - 9 do not change with different values of l, but the scale of the x-axis. If the BSs are deployed in an area of, e.g., 100m x 100m, Figs. 5 - 9 should be read with the x-axis label "Power loss coefficient per 100 meters".

A. Different DDPL Values

Fig. 5: Average total power drawn from the main grid of the MF algorithm ($M^{\text{MF\_CNG}}$) and the MCMF algorithm ($M^{\text{MCMF\_CNG}}$) versus power loss coefficient per l meters.

Fig. 5 shows the average total power drawn from the main grid of the MF algorithm ($M^{\text{MF\_CNG}}$) and the MCMF algorithm ($M^{\text{MCMF\_CNG}}$) versus power loss coefficient per l meters (C) by a dashed gray line and a solid gray line, respectively. Simulation values are derived by running the two proposed algorithms and are depicted by lines on the left side of the legend whereas the corresponding analytical values are calculated with the formulas in Section V and are depicted by markers on the right side of the legend. The three analytically derived values lie exactly on the corresponding lines of the simulation values, which proves the correctness of our closed-form expressions in Section V.

The MCMF algorithm saves more grid power than the MF algorithm for any given $C > 0$ because it takes into account the power loss in the transmission lines in the optimization. As a result, the power flow in the network travels over shorter distances in the MCMF algorithm and is therefore subject to a smaller power loss than in the MF algorithm. The performance gap (Δ) between the two algorithms is greater for moderate C than for very large or very small C. Hence, the higher complexity of running an MCMF algorithm compared to an MF algorithm can be justified if C is moderate. Because no power is lost in the transmission lines for $C = 0$, $M^{\text{MF\_CNG}}$ is equal to $M^{\text{MCMF\_CNG}}$, $M_1^{\text{MF\_CNG}}$, and $M_1^{\text{MCMF\_CNG}}$ (circle in Fig. 5).

$M^{\mathrm{MF\_CNG}}$ and $M^{\mathrm{MCMF\_CNG}}$ are bounded by the dashed black horizontal lower bound line corresponding to the $M_1^{\mathrm{MF\_CNG}} = M_1^{\mathrm{MCMF\_CNG}}$ value and the solid black horizontal upper bound line corresponding to the $M^{\mathrm{MF\_ENG}} = M^{\mathrm{MCMF\_ENG}}$ value. The lower and upper bound are horizontal lines, because $M_1^{\mathrm{MF\_CNG}}$, $M_1^{\mathrm{MCMF\_CNG}}$, $M^{\mathrm{MF\_ENG}}$, and $M^{\mathrm{MCMF\_ENG}}$ are independent of C. These two horizontal lines correspond to the extreme points of the cellular network behavior where all BSs behave like one single mega BS corresponding to the dashed black horizontal line in Fig. 5 and all BSs behave like isolated BSs corresponding to the solid black horizontal line in Fig. 5.

The power, which cannot be balanced out in the network and therefore flows on the virtual (s,t) edge, is the same in both algorithms. Hence, $M_1^{\mathrm{MF\_CNG}}$ is equal to $M_1^{\mathrm{MCMF\_CNG}}$. The total power drawn from the main grid on an edgeless neighboring graph is the same in both algorithms. Hence, $M^{\mathrm{MF\_ENG}}$ is equal to $M^{\mathrm{MCMF\_ENG}}$.

B. Different BS Densities

Fig. 6 shows the performance of both algorithms for different numbers of BSs (N). The performance gap (Δ) between the two algorithms increases with the number of BSs, i.e., a denser cellular network. This is because a denser cellular network offers more opportunities for power sharing between BSs, and the power savings from minimizing the distances traveled by the power flows become more significant. The MCMF algorithm saves up to 10%, 22% and 30% more power than the MF algorithm for $N = 5$, $N = 10$ and $N = 15$ BSs, respectively. The BSs density influences significantly Δ.

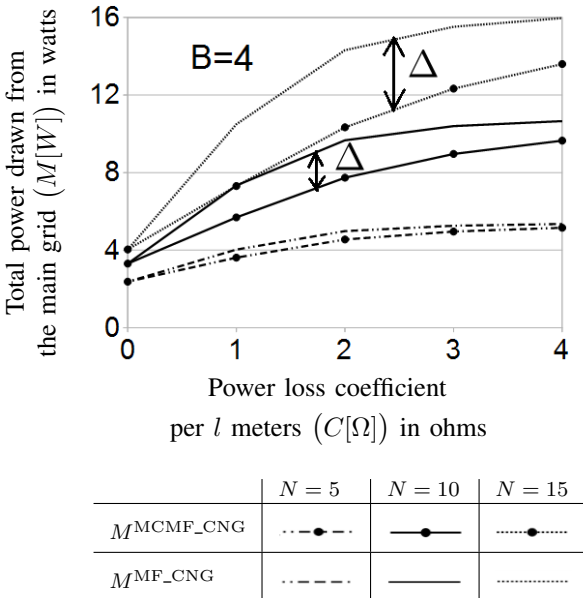|	$N=5$	$N=10$	$N=15$
$M^{\mathrm{MCMF\_CNG}}$	$\cdot\cdot\!-\!\bullet\!-\!\cdot\cdot$	$\text{---}\!\bullet\!\text{---}$	$\cdots\!\bullet\!\cdots$
$M^{\mathrm{MF\_CNG}}$	$\cdot\cdot\!-\!-\!\cdot\cdot$	--------	$\cdots\cdots\cdots$

Fig. 6: Average total power drawn from the main grid of the two proposed algorithms versus power loss coefficient per l meters for different number of BSs (N).

C. Different Maximum Power Surpluses/Deficits

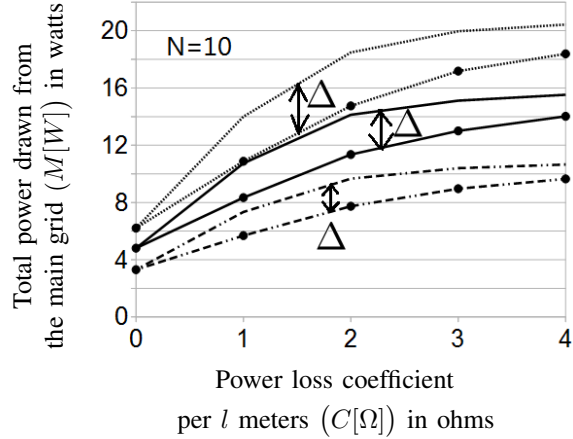|	$B=4$	$B=6$	$B=8$
$M^{\mathrm{MCMF\_CNG}}$	$\cdot\cdot\!-\!\bullet\!-\!\cdot\cdot$	$\text{---}\!\bullet\!\text{---}$	$\cdots\!\bullet\!\cdots$
$M^{\mathrm{MF\_CNG}}$	$\cdot\cdot\!-\!-\!\cdot\cdot$	--------	$\cdots\cdots\cdots$

Fig. 7: Average total power drawn from the main grid of the two proposed algorithms versus power loss coefficient per l meters for different maximum power surpluses/deficits (B).

Fig. 7 shows the performance of both algorithms for different maximum power surpluses/deficits (B). Greater maximum power surplus/deficit values (B) happen if the maximum power generation rises, e.g., due to solar cells with a greater surface area, and if the maximum power consumption rises, e.g., due to more UEs connected to the BSs. If the B value rises, the average total power drawn from the main grid rises in both algorithms, but the relative performance gap between the two algorithms is constant. In other words, The MCMF algorithm saves up to 22% more power than the MF algorithm for all three cases: $B = 4$, $B = 6$ and $B = 8$. This can be explained by the fact that the power, which cannot be balanced out in the network and therefore flows on the virtual (s,t) edge, is the same in both algorithms. Hence, $M_1^{MF\_CNG}$ is equal to $M_1^{MCMF\_CNG}$. The performance gap (Δ) between the two algorithms is only caused by the difference between the $M_2^{MF\_CNG}$ value and the $M_2^{MCMF\_CNG}$ value. In other words, the performance gap (Δ) is only caused by the fact that the MF algorithm losses more power during the transmission due to longer transmission distances. For the investigated cellular network with $N = 10$ BSs, the power loss aware MCMF algorithms saves up to 22% more power than the power loss unaware MF algorithm.

D. Different Power Surplus/Deficit Distributions

To extend the considered cellular network scenarios, we will evaluate the effects of different discrete uniform distributions and of different binomial distributions for the B_i values in the following paragraph.
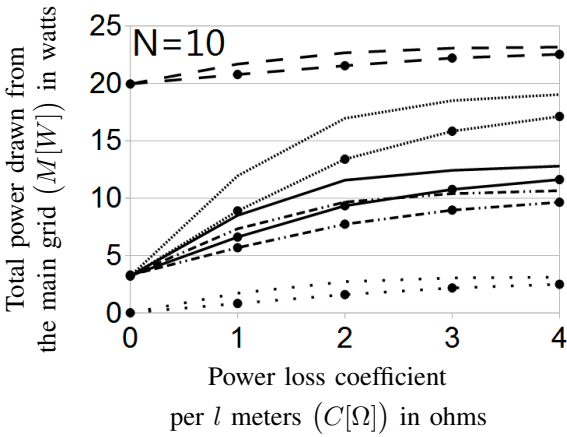
We denote the discrete uniform distribution of the integers in the interval $[a, b]$ as $U[a, b]$. Each integer in the interval is equally likely to be observed. The investigated uniform distributions are given in Fig. 10. The uniform distributions with ID 1, ID 2, ID 3, ID 4, and ID 5 are the uniform distributions $U[-4, 4]$ shifted +4, +2, 0, -2, -4 along the x-axis (cf. Fig. 10), respectively.

We denote the binomial distribution with parameters $\tilde{n}$ and $\tilde{p}$ as $Bin(\tilde{n}, \tilde{p})$. The probability of B_i having the value k in a binomial distribution is given as:

$$\mathbb{P}(B_i = k) = \binom{\tilde{n}}{k} \tilde{p}^k (1 - \tilde{p})^{\tilde{n}-k} \quad k \in \{0, 1, ..., \tilde{n}\}. \quad (33)$$

The investigated binomial distributions are given in Fig. 11. The binomial distributions with ID 6, ID 7, ID 8, ID 9, and ID 10 are the binomial distributions $Bin(8, 0.5)$ shifted 0, -2, -4, -6, -8 along the x-axis (cf. Fig. 11), respectively. We set the parameter $\tilde{n} = 8$ so that all distributions in Figs. 10 - 11 have the same support. We set the parameter $\tilde{p} = 0.5$ so that the binomial distributions are symmetrical similar to the energy generation profile of a solar cell.

Fig. 8 and Fig. 9 evaluate uniform distributions and binomial distributions, respectively. The absolute values in Fig. 8 are different to the absolute values in Fig. 9 due to the different types of distributions but the general shape of the curves are similar in both figures.
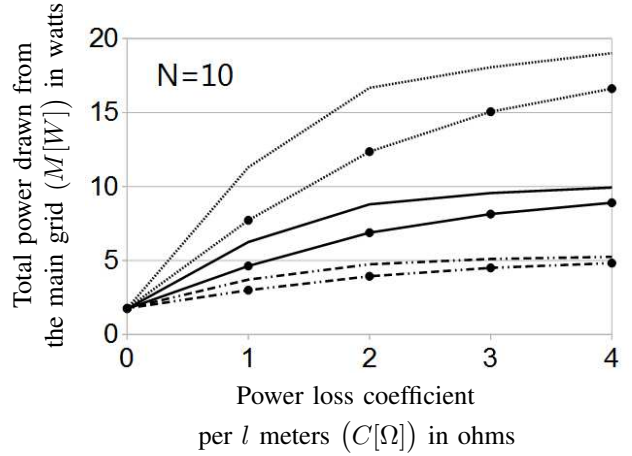
Fig. 9: Average total power drawn from the main grid of the two proposed algorithms versus power loss coefficient per l meters for different distributions IDs from Fig. 11.

1) Different Power Surplus/ Deficit Value Distributions In One Cellular Network: ID 1/5 and ID 2/4 in Fig. 8 and ID 6/10 and ID 7/9 in Fig. 9 evaluate cellular network scenarios where the power surplus/deficit values B_i do not follow the same distribution among all BSs, i.e., the B_i values of half of the BSs follow the first distribution whereas the B_i values of the other half of the BSs follow the second distribution.

2) Match/Mismatch Between The Total Power Surplus And The Total Power Deficit: The slopes of ID 2 and ID 4 are smaller than the slope of ID 3 in Fig 8. This shows that more power is shared in the cellular network with power distribution ID 3, because the total power surplus and the total power deficit on average is the same for ID 3. BSs with power distributions ID 2 and ID 4 have more likely a power surplus and a power deficit, respectively.

3) High/Low Fluctuations Of The Power Surplus And Power Deficit Values: ID 1/5 in Fig. 8 and ID 6/10 in Fig. 9 have a high fluctuation of the power surplus and power deficit values. ID 2/4 in Fig. 8 and ID 7/9 in Fig. 9 have a medium fluctuation of the power surplus and power deficit values. ID 3 in Fig. 8 and ID 8 in Fig. 9 have a low fluctuation of the power surplus and power deficit values. The higher the fluctuation the more power is shared in the cellular network and the more power is lost in the transmission lines.

4) Harvesting Devices Are Not Present On All The BSs: ID 1/5 in Fig. 8 and ID 6/10 in Fig. 9 evaluate cellular network scenarios where the harvesting devices are not present on all the BSs, because half of the BSs follow the distributions ID 5 or ID 10, respectively. BSs following distributions ID 5 or ID 10 have no power surplus, hence there are no harvesting devices present at these BSs.

Fig. 8: Average total power drawn from the main grid of the two proposed algorithms versus power loss coefficient per l meters for different distributions IDs from Fig. 10.
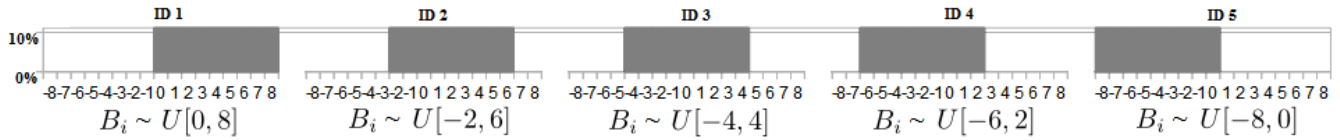
Fig. 10: Probability mass functions of the uniform distributions with ID 1 - 5
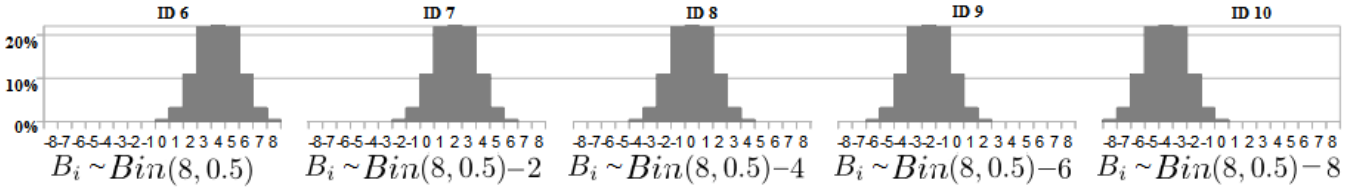

Fig. 11: Probability mass functions of the binomial distributions with ID 6 - 10

5) Different Capacities/Sizes Of Energy Harvesters: ID 1 and ID 2 in Fig. 10 as well as ID 6 and ID 7 in Fig. 11 have a harvesting device of a large size, because it is more likely that these BSs experience a power surplus. ID 3 in Fig. 10 and ID 8 in Fig. 11 have a harvesting device of a medium size, because it is equally likely that these BSs experience a power surplus or deficit. ID 4 and ID 5 in Fig. 10 as well as ID 9 and ID 10 in Fig. 11 have a harvesting device of a small size, because it is more likely that these BSs experience a power deficit.

VII. CONCLUSION

We have developed an MF algorithm and an MCMF algorithm to optimize the sharing of renewable power among BSs with the objective of minimizing the total power drawn from the main grid by the BSs. The MCMF algorithm has a higher computational complexity but results in a more efficient use of the harvested power because it minimizes the DDPL in the transmission lines by sharing renewable power among nearby BSs wherever possible. We have derived a closed-form expression of the average total power drawn from the main grid by the BSs for the MF algorithm. Our simulation results on a complete neighboring graph, i.e., every BS can share power with every other BS in the network, have shown that our derived closed-form expression for the MF algorithm is accurate, and that the power saving gain (Δ) of the MCMF algorithm over the MF algorithm depends on the power loss coefficient (C) per l ($\in \mathbb{R}^+$) meters of transmission line. On the one hand, Δ converges to 0% if C is very large or very small. In such cellular networks, the simpler MF algorithm should be used. On the other hand, for cellular networks with a moderate C, Δ increases with the BS density. In such cellular networks, the MCMF algorithm saves up to 10%, 22%, and 30% more main grid power than the MF algorithm for 5, 10 and 15 BSs uniformly distributed in a square area of l^2 square meters, respectively.

REFERENCES

[1] D. Benda, X. Chu, S. Sun, T. Q. Quek, and A. Buckley, "Modeling and optimization of energy sharing among base stations as a minimum-cost-maximum-flow problem," in *Proc. IEEE VTC-Spring*, Porto, Portugal, Jun 2018, pp. 1–5.

[2] A. Kwasinski and A. Kwasinski, "Increasing sustainability and resiliency of cellular network infrastructure by harvesting renewable energy," *IEEE Communications Magazine*, vol. 53, no. 4, pp. 110–116, Apr 2015.

[3] Y. Mao, Y. Luo, J. Zhang, and K. B. Letaief, "Energy harvesting small cell networks: feasibility, deployment, and operation," *IEEE Communications Magazine*, vol. 53, no. 6, pp. 94–101, Jun 2015.

[4] D. Benda, S. Sun, X. Chu, T. Q. S. Quek, and A. Buckley, "PV cell angle optimization for energy generation-consumption matching in a solar powered cellular network," *IEEE Transactions on Green Communications and Networking*, vol. 2, no. 1, pp. 40–48, Mar 2018.

[5] X. Huang and N. Ansari, "Energy sharing within EH-enabled wireless communication networks," *IEEE Wireless Communications*, vol. 22, no. 3, pp. 144–149, Jun 2015.

[6] Y. Guo, L. Duan, and R. Zhang, "Optimal pricing and load sharing for energy saving with cooperative communications," *IEEE Transactions on Wireless Communications*, vol. 15, no. 2, pp. 951–964, Feb 2016.

[7] M. J. Farooq, H. Ghazzai, A. Kadri, H. ElSawy, and M. S. Alouini, "A hybrid energy sharing framework for green cellular networks," *IEEE Transactions on Communications*, vol. 65, no. 2, pp. 918–934, Feb 2017.

[8] M. J. Farooq, H. Ghazzai, A. Kadri, H. ElSawy, and M. S. Alouini, "Energy sharing framework for microgrid-powered cellular base stations," *IEEE Global Communications Conference*, pp. 1–7, Dec 2016.

[9] A. F. Crossland, O. H. Anuta, and N. S. Wade, "A socio-technical approach to increasing the battery lifetime of off-grid photovoltaic systems applied to a case study in Rwanda," *Renewable Energy*, vol. 83, pp. 30 – 40, Nov 2015.

[10] Y. K. Chia, S. Sun, and R. Zhang, "Energy cooperation in cellular networks with renewable powered base stations," *IEEE Transactions on Wireless Communications*, vol. 13, no. 12, pp. 6996–7010, Dec 2014.

[11] CelPlan. (2014) White paper - customer experience optimization in wireless networks. [Online]. Available: http://www.celplan.com/resources/whitepapers/Customer%20Experience%20Optimization%20rev3.pdf

[12] R. K. Ahuja, M. Kodialam, A. K. Mishra, and J. B. Orlin, "Computational investigations of maximum flow algorithms," *European Journal of Operational Research*, vol. 97, no. 3, pp. 509–542, Mar 1997.

[13] J. Vygen, "On dual minimum cost flow algorithms," *Mathematical Methods of Operations Research*, vol. 56, no. 1, pp. 101–126, Aug 2002.

[14] X. Huang, T. Han, and N. Ansari, "Smart grid enabled mobile networks: Jointly optimizing BS operation and power distribution," *IEEE/ACM Transactions on Networking*, vol. 25, no. 3, pp. 1832–1845, Jun 2017.

[15] H. Cole and D. Sang, *Revise AS Physics for AQA A*. Oxford, United Kingdom: Heinemann Educational Publishers, 2001, pp. 67–68.

[16] B. Korte and J. Vygen, *Combinatorial Optimization: Theory and Algorithms*, 5th ed. Germany: Springer-Verlag Berlin Heidelberg, 2012, p. 177.

[17] E. W. Weisstein. (2008) Dice from MathWorld–A Wolfram Web Resource. [Online]. Available: http://mathworld.wolfram.com/Dice.html

[18] P. Fan, G. Li, K. Cai, and K. B. Letaief, "On the geometrical characteristic of wireless Ad-Hoc networks and its application in network performance analysis," *IEEE Transactions on Wireless Communications*, vol. 6, no. 4, pp. 1256–1265, Apr 2007.

[19] Z. Khalid and S. Durrani, "Distance distributions in regular polygons," *IEEE Transactions on Vehicular Technology*, vol. 62, no. 5, pp. 2363–2368, Jun 2013.

[20] U. Bäsel, "Random chords and point distances in regular polygons," *Acta Mathematica Universitatis Comenianae*, vol. 83, no. 1, pp. 1–18, May 2014.

[21] E. W. Weisstein. (2017) Square Line Picking from MathWorld–A Wolfram Web Resource. [Online]. Available: http://mathworld.wolfram.com/SquareLinePicking.html

Doris Benda (S'17) received the B.Sc. degree in Mathematics from the University of Bonn (Germany) in 2014 and the M.Sc. degree from the Liverpool John Moores University (United Kingdom) in 2015. Currently, she is pursuing the Ph.D. degree in Electrical Engineering at the University of Sheffield (United Kingdom). Since 2016, she is with the Institute for Infocomm Research (Singapore). Her research interests span various areas in green communication and network optimization, especially the incorporation of renewable energy in the cellular network. She is an awardee of the A*STAR Research Attachment Programme between Singapore and Sheffield.

Xiaoli Chu (M'06-SM'15) is a Reader in the Department of Electronic and Electrical Engineering at the University of Sheffield, UK. She received the B.Eng. degree in Electronic and Information Engineering from Xi'an Jiao Tong University in 2001 and the Ph.D. degree in Electrical and Electronic Engineering from the Hong Kong University of Science and Technology in 2005. From 2005 to 2012, she was with the Centre for Telecommunications Research at King's College London. Xiaoli has co-authored over 100 peer-reviewed journal and conference papers. She is co-recipient of the IEEE Communications Society 2017 Young Author Best Paper Award. She is the lead editor/author of the book "Heterogeneous Cellular Networks - Theory, Simulation and Deployment" published by Cambridge University Press (May 2013) and the book "4G Femtocells: Resource Allocation and Interference Management" published by Springer (November 2013). She is Editor for the IEEE COMMUNICATIONS LETTERS and the IEEE WIRELESS COMMUNICATIONS LETTERS. She was Guest Editor for the IEEE TRANSACTIONS ON VEHICULAR TECHNOLOGY and the ACM/Springer Journal of Mobile Networks & Applications. She was Co-Chair of Wireless Communications Symposium for the IEEE International Conference on Communications (ICC) 2015, Workshop Co-Chair for the IEEE International Conference on Green Computing and Communications 2013, and has been Technical Program Committee Co-Chair of 6 workshops on heterogeneous and small cell networks for IEEE ICC, GLOBECOM, WCNC, and PIMRC.

Sumei Sun (F'16) is currently the Head of the Communications and Networks Cluster, Institute for Infocomm Research, Agency for Science, Technology, and Research, Singapore, focusing on smart communications and networks for robust, QoS/QoE-guaranteed, and energy- and spectrum-efficient connectivity for human, machine, and things. She has authored or co-authored over 200 technical papers in prestigious IEEE journals and conferences, and holds 30 granted patents and over 30 pending patent applications, many of which have been licensed to industry. She is a Distinguished Lecturer of the IEEE Vehicular Technology Society 2014-2018, a Distinguished Visiting Fellow of the Royal Academy of Engineering, U.K., in 2014, and Vice Director of IEEE Communications Society Asia Pacific Board since 2016. She has also been actively contributing to organizing IEEE conferences in different roles, including her recent services as Executive Vice Chair of Globecom 2017, Symposium Co-Chair of ICC 2015 and 2016, Track Co-Chair of IEEE VTC 2016 Fall, VTC 2017 Spring, etc. She was an Editor of the IEEE TRANSACTIONS ON VEHICULAR TECHNOLOGY (TVT) during 2011-2017, and Editor of the IEEE WIRELESS COMMUNICATION LETTERS during 2011-2016. She serves as an Area Editor of IEEE TVT since July 2017, and Editor of the IEEE COMMUNICATIONS SURVEYS AND TUTORIALS, since 2015. She received the "***Top Associate Editor***" award in 2011, 2012, and 2015, all from IEEE TRANSACTIONS ON VEHICULAR TECHNOLOGY.

Tony Q.S. Quek (S'98-M'08-SM'12-F'18) received the B.E. and M.E. degrees in electrical and electronics engineering from the Tokyo Institute of Technology, Tokyo, Japan, in 1998 and 2000, respectively, and the Ph.D. degree in electrical engineering and computer science from the Massachusetts Institute of Technology, Cambridge, MA, USA, in 2008. Currently, he is a tenured Associate Professor with the Singapore University of Technology and Design (SUTD). He also serves as the Acting Head of ISTD Pillar and the Deputy Director of the SUTD-ZJU IDEA. His current research topics include wireless communications and networking, internet-of-things, network intelligence, wireless security, and big data processing.

Dr. Quek has been actively involved in organizing and chairing sessions, and has served as a member of the Technical Program Committee as well as symposium chairs in a number of international conferences. He is currently an elected member of IEEE Signal Processing Society SPCOM Technical Committee. He was an Executive Editorial Committee Member for the IEEE TRANSACTIONS ON WIRELESS COMMUNICATIONS, an Editor for the IEEE TRANSACTIONS ON COMMUNICATIONS, and an Editor for the IEEE WIRELESS COMMUNICATIONS LETTERS. He is a co-author of the book "Small Cell Networks: Deployment, PHY Techniques, and Resource Allocation" published by Cambridge University Press in 2013 and the book "Cloud Radio Access Networks: Principles, Technologies, and Applications" by Cambridge University Press in 2017.

Dr. Quek was honored with the 2008 Philip Yeo Prize for Outstanding Achievement in Research, the IEEE Globecom 2010 Best Paper Award, the 2012 IEEE William R. Bennett Prize, the 2015 SUTD Outstanding Education Awards – Excellence in Research, the 2016 IEEE Signal Processing Society Young Author Best Paper Award, the 2017 CTTC Early Achievement Award, the 2017 IEEE ComSoc AP Outstanding Paper Award, and the 2017 Clarivate Analytics Highly Cited Researcher. He is a Distinguished Lecturer of the IEEE Communications Society and a Fellow of IEEE.
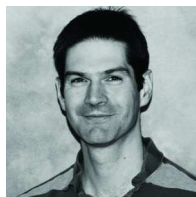
Alastair Buckley is a senior lecturer in organic electronics and photonics at the University of Sheffield. He moved to academia in 2008 following 8 years industrial R&D in polymer light emitting display device development and manufacturing with MicroEmissive Displays PLC. At University he has expanded his research to include organic PV devices and also interdisciplinary studies of the widespread integration of PV into society. This new research direction has resulted in improved understanding the performance of UK based PV systems and how PV integrates into the energy system. He leads UK web based PV monitoring and forecasting services that have been developed to address the growing need of the UK energy sector to better manage its diversifying energy portfolio. https://www.solar.sheffield.ac.uk/pvlive/